Dear reviewers,
Thank you for your effort and constructive comments.

Reviewer 1 comments:

1- In the abstract, it is noted that one neuroradiologist and another radiologist reported the CTA, but in the method, it is written that two neuroradiologists reviewed the images.
Reply: Two neuroradiologists reviewed the images. Modifications were done.

2- The submission needs native English editing.
Reply: Manuscript was edited by professional editing service.

3- Why was DSA performed in 80 patients? The indication for doing brain DSA is not mentioned.
Reply: It was requested by neurosurgeon and neuro-interventionist as a part of management plan.

4- Certainly, the two neuroradiologists who reviewed the images are experienced and skilled, but to draw a conclusion, I think more physicians qualified in neuroimaging should review the images.
Reply: Unfortunately, the current study was limited to two neuroradiologist only. It was listed as a limitation, and we recommend a future study to evaluate the diagnostic accuracy of CTA by radiologists, neurologists, and neuro-interventionists.

5- Rewriting the article by focusing on the role of CTA in the aneurysmal SAH.
Reply: The role of CTA in the aneurysmal SAH was added to introduction and discussion.

Inter-observer reliability of CT angiography in the assessment of ruptured intracranial aneurysm features and impact on patient management

ABSTRACT

Background: Aneurysmal subarachnoid hemorrhage (SAH) is an emergency that can lead to a high mortality rate and many severe complications. It is critical to make a rapid radiological evaluation of ruptured intracranial aneurysms to determine the appropriate surgical treatment.

Aim: To assess the reliability of CT angiography (CTA) in assessing different features of ruptured intracranial aneurysm and its impact on patient management.

Methods: The final cohort of this study consisted of 146 patients with ruptured intracranial aneurysms (75 male and 71 female) who underwent cerebral CTA. Their age ranged from 25 to 80, and the mean age ± SD was 57±8.95 years. Two readers were asked to assess different features related to the aneurysm and perianeurysmal environment. Inter-observer agreement was measured using kappa statistics. Imaging data extracted from NCCT and CTA were considered to categorize the study population into two groups according to the recommended therapeutic approach.

Results: The inter-observer agreement of both reviewers was excellent for the detection of aneurysms (K= 0.95, P=0.001), aneurysm location (K= 0.98, P=0.001), & (K= 0.98, P=0.001), morphology (K= 0.92, P=0.001) and margins (K= 0.95, P=0.001). There was an excellent interobserver agreement for the measurement of aneurysm size (K= 0.89, P=0.001), neck (K= 0.85, P=0.001), and dome-to-neck ratio (K= 0.98, P=0.001). There was an excellent inter-observer agreement for the detection of other aneurysm-related features such as thrombosis (K= 0.82, P=0.001), calcification (K= 1.0, P=0.001), bony landmark (K= 0.89, P=0.001) and branch incorporation (K= 0.91, P=0.001) as well as perianeurysmal findings including vasospasm (K= 0.91, P=0.001), perianeurysmal cyst (K= 1.0, P=0.001) and associated vascular lesions (K= 0.83, P=0.001). Based on imaging features, 87 patients were recommended to have endovascular treatment, while surgery was recommended in 59 patients. 71.2 % of the study population underwent the recommended therapy.

Conclusions: CTA is a reproducible promising diagnostic imaging modality for detecting and characterizing cerebral aneurysms.

Keywords: CT angiography; intracranial aneurysm; subarachnoid hemorrhage; intracranial hemorrhage; Observer variation

INTRODUCTION

Acute subarachnoid hemorrhage (SAH) is a medical emergency that can lead to a high mortality rate and many severe complications. The most frequent cause of non-traumatic subarachnoid hemorrhage is a ruptured aneurysm. Ruptured aneurysms not only cause subarachnoid bleeding but can also cause subdural or intracerebral hematomas. It is critical to make a rapid radiological evaluation of ruptured intracranial aneurysms to determine the appropriate surgical treatment of SAH **(1).** Different imaging modalities are used or have been used to assess intracranial vascular lesions. Digital subtraction angiography (DSA) has been considered the "gold standard" for detecting intracranial aneurysms and therapeutic decision-making. Additionally, intra-arterial cone beam CT angiography (CTA) using flat panel detector incorporates the high spatial vascular resolution of 3D rotational angiography with CT postprocessing techniques to increase the contrast resolution **(2)**. Nevertheless, it is an invasive and time-consuming technique with a reported 0.5% risk of neurological complications **(3).** MR angiography enables visualization of intra-cranial arteries without ionizing radiation or intravenous contrast material. The performance of MR angiography in evaluating acute subarachnoid hemorrhage also has been compared favorably with that of DSA. However, MR angiography can be technically challenging for acutely ill patients. Additionally, aneurysms less than 5 mm in diameter might be missed in MRA studies**(4).**

Compared to DSA, CTA is a safe, relatively inexpensive, and noninvasive imaging. CT angiography is not associated with significant patient risks other than those related to administering iodinated contrast media. Images can be relatively safely obtained without the need for arterial puncture or catheter manipulation that carries the possibility of acquiring a permanent neurologic deficit **(5*).*** For these reasons, helical cerebral CT angiography has been widely used in detecting intracranial aneurysms, with a reported sensitivity of 70–96% **(6).** Currently, multidetector CT angiography has the ability to detect most intracranial aneurysms of 5 mm or larger. Multidetector row CT scanners provide increased spatial resolution and decreased scanning time, which should increase the sensitivity of the technique in depicting aneurysms of less than 5 mm in diameter**.** Currently, CT angiography is accepted as a first-line diagnostic imaging modality for evaluating intracranial aneurysms. Nevertheless, using CT

angiography to depict intracranial aneurysms showed variable sensitivity. The reported sensitivity of CTA in detections of small intracranial aneurysms (<3 mm) varied from 28%–43% in a study that included 99 small aneurysms **(7)** to 83-92 % in another study had 579 small aneurysms **(8)**.

Deciding whether to perform surgical clipping or endovascular therapy for an intracranial aneurysm is vital. Treatment of intracranial aneurysms depends on clinical features, including age, Hunt and Hess grade, neurological or medical comorbidity, and characters of the aneurysm itself. Advances in imaging technologies have improved our comprehension of the three-dimensional (3D) geometry of cerebral aneurysms, which has further affected treatment procedures, and helps neurosurgeons in the diagnosis, planning, and assessment of the therapeutic modalities**.** Exact information must be obtained preoperatively regarding the location, size, and morphology of the aneurysm and the property of the aneurysmal wall, its relationship with the parent vessel and adjacent branches, vessel incorporation, presence of calcification or thrombus **(9)**. Perianeurysmal information such as associated vasospasm, vascular variants, presence of vascular malformations, and the relationship of the aneurysm to the bony skull base is also crucial for proper treatment method selection.

This work aims to assess the inter-observer reliability of CT angiography (CTA) in assessing different features of ruptured intracranial aneurysms and their impact on patient management.

MATERIAL AND METHODS

Study population

The Institutional review board approved this single-center prospective study. One hundred sixty-one consecutive patients with clinically suspected intracranial aneurysms were recruited. Inclusion criteria were adult patients with imaging signs of subarachnoid hemorrhage by non-enhanced CT. The exclusion criteria were patients with renal insufficiency (n = 6), pregnant or lactating females (n = 2), and non-diagnostic examinations (n = 7). The final cohort of our study included 146 patients (75 male and 71 female). Their age ranged from 25 to 80 years, with a mean age was 57±8.9 years. Once enrolled, all patients were submitted to a contrast-enhanced CTA scan for diagnosis of intracranial aneurysm. The commonest clinical presentation was headache, neck pain, and depressed consciousness in 130 patients, hemiparesis in 12 patients, cranial nerve palsies, and blurring of vision being less common presenting symptoms in 3 patients. One patient presented in an accident. The flow chart of our study is illustrated in **(Fig. 1)**.

CTA Technique

All examinations were carried out with 160-slice computed tomography (Toshiba Aquilion Prime 160, Tochigi, Japan). Examinations were performed in a supine position with the arms of the patients beside the body. We first performed a non-contrast CT (NCCT) scan of the whole brain in an axial plane tilted along the occipito-meatal line using the following parameters: tube voltage 100 kVp, FOV 220 mm, collimation 0.75 mm, matrix size 512 × 512, slice thickness 3.0 mm, and rotation time 1.0 s. CTA examinations were achieved using the bolus triggering technique for the timing of contrast medium injection. An ROI was centered at the upper end of the common carotid artery and sized to include only the lumen of the artery. The bolus triggering technique started automatically after contrast-medium injection when an attenuation value of 100 HU was reached in ROI. Non-ionic contrast medium Ultravist 370 (370 mgI/ml, Bayer Healthcare Ltd, Guangzhou, China) at a dose of 1 mL/Kg and rate of 4mL/sec followed by a 50 mL saline flush administered via automatic injector (Medrad Stellent, Warrendale, PA) through a 20 G intravenous cannula in the antecubital fossa of either upper extremity. The following parameters were used: tube voltage 120 kVp, automatic tube current modulation, FOV 250 mm,

collimation 0.75 mm, matrix size 512 × 512, slice thickness 1.5 mm, rotation time 0.3 s. Scanning was performed in the caudocranial direction and started at the level of the aortic arch up to the vertex. Axial images were stored and transferred into the workstation as source images after reconstruction at 0.625-mm intervals. Multiplanar reformats (MPR), maximum intensity projection (MIP), and 3D volume-rendered images were used for further analysis.

Image analysis

Image analysis was conducted on the PACS system (GE Healthcare, Waukesha, WI). All CTA examinations were revised and interpreted by two experienced neuroradiologists with 14 and 8 years of experience in neurovascular imaging (AHE, BE). They independently reviewed the images blinded to patient data and final diagnosis. The following features obtained at NCCT were individually evaluated for each patient: The degree of SAH using the Fisher scale, associated parenchymal hemorrhage, hydrocephalus, and ischemic changes. Both readers were asked to predict the location of the aneurysm based on the distribution of SAH and IPH. At CTA, both readers were asked to evaluate the following aneurysm features': (i) number, (ii) size, (iii) location (anterior vs. posterior circulation, parent artery, and affected segment), (iv) shape (saccular, fusiform, serpentine or blister), (v) margin (sharp, irregular / daughter sacs) (vi) presence of calcification and/or thrombus, (vii) the presence of branch incorporation and (viii) the orientation of the aneurysm in relation to the parent vessel (e.g., pointing superior/inferior, medial/lateral, anterior/posterior). Aneurysm size was defined by the maximum measurement of aneurysm width, neck width (the largest cross-sectional diameter of the aneurysm neck), depth (the longest diameter between the neck and dome), and aneurysm neck-to-dome length. According to size, aneurysms were classified into (i) small aneurysms are less than 5 mm, (ii) medium-sized aneurysms are 6–15 mm, (iii) large aneurysms are 16–25 mm, and (iv) giant aneurysms are > 25 mm. The following features related to the perianeurysmal environment were evaluated by both readers: (i) associated vasospasm, (ii) perianeurysmal cysts, (iii) associated vascular malformations (type and classification based on relation to aneurysm), (iv) vascular variants, and (v) the relationship of the aneurysm to the bony landmarks or related osseous changes (remodeling or fractures).

Management selection:

Imaging data extracted from NCCT and CTA were considered to categorize the study population into two groups according to the recommended therapeutic approach. The first group was recommended to proceed to endovascular therapy, and the second group was advised to undergo surgical management (clipping). **Features in favor of endovascular therapy (coiling) were:** (i) absence of parenchymal hematoma, (ii) posterior circulation aneurysm, (iii) small aneurysm neck < 4 mm, (iv) aneurysm diameter < 15 mm and (v) unilobar shape, (vi) multiple aneurysms, (vii) calcification located at the aneurysm neck that might interfere with clipping and (viii) presence of vasospasm. Coiling using balloon remolding technique or stent-assisted coiling was recommended with wide-neck aneurysms. **Features favored surgical management (clipping) were** (i) presence of intra-parenchymal hematoma, (ii) middle cerebral and pericallosal arteries aneurysm, (iii) wide neck of the aneurysm > 4 mm, (iv) aneurysm diameter > 15 mm, (v) abnormal configuration unsuitable for endovascular therapy, (vi) aneurysmal sac incorporating arterial branches (vii) presence of intraluminal thrombus and (viii) vascular variant interferes with endovascular management. Features considered in managing ruptured intracranial aneurysms are listed in **Table (1).**

Statistical analysis:

All statistical analyses were performed with software (SPSS, version 16.0; SPSS, Chicago, Ill). The Kolmogorov-Smirnov Z-test was used to test the normality of the continuous variable groups. The CTA image quality scores were ranked and listed as a mean and standard deviation. The kappa statistic (K), including a 95% confidence interval (CI) with an intra-class correlation (r), was used to estimate the proportion of interobserver agreement beyond that expected by chance for the image quality grading and depiction of the aneurysm, its neck, parent artery, and associated anomalies. A (P) value less than 0.05 was considered to indicate a statistically significant difference. The K values were interpreted as follows: k values between 0.61 and 0.80 represented good; k values between 0.81 and 1.00 represented excellent agreement.

RESULTS

NCCT findings

Both readers used the Fisher scale to assess SAH. The means scores were (3.47±0.6 and 3.33±0.4) with a good interobserver agreement (K= 0.79, P=0.001). Excellent interobserver agreement between both readers in the detection of IPH (K= 0.1, P=0.001) as well as in the detection of hydrocephalus (K= 0.92, P=0.001). A statistically significant strong positive correlation was found between the location of SAH and IPH on NCCT scan and the eventual location of a ruptured cerebral aneurysm in single ones and as a differentiating point of culprit aneurysm in multiple aneurysms confirmed by CTA & surgical or endovascular intervention. The sensitivity of NCCT predicting aneurysms depends on blood distribution of more than 85% in our study. **Table (2)** shows the inter-observer results of CT and CTA findings**.**

Aneurysm characters:

Detection: The first reader detected 166 aneurysms (126 single aneurysms (75.9%) and 40 multiple aneurysms (24.1%)), while 2nd reader detected 169 aneurysms (127 single aneurysms (75.1%) and 42 multiple aneurysms (24.9%)). An excellent interobserver agreement was found between both readers in detecting an aneurysm (98.8% (K= 0.95, P=0.001)). Among multiple aneurysms, 14 were mirror image aneurysms (MA), and the remaining were non-mirror image (NMA). The commonest location of MA in our series was the M1 segment or at the MCA bifurcation (n=3), followed by the cavernous portion of ICA (n=2) **(fig.2)**, the PCom (n=1), and ICA terminus (n=1). The sensitivity of CTA compared to DSA in the detection of intracranial aneurysms was 98.8%. DSA identified 89 aneurysms in 80 patients. Among these aneurysms, CTA failed to detect one in a patient with three other aneurysms. The missed aneurysm was located in (PCA) with diameters of 3mm. In two cases, CTA depicted aneurysms, which DSA missed. An ICA blister and a distal MCA mycotic aneurysm were the two missed aneurysms.

Location: For most of the study, the population was harboring anterior circulation aneurysms (94%). Excellent interobserver agreement was found between both readers in the detection of aneurysms in the anterior and posterior circulation (K= 0.95, P=0.001) as well as its site in parent

artery & segment (K= 0.98, P=0.001), & (K= 0.98, P=0.001). In this study, Acom was the most affected artery, and Acom-left ACA complex was the most affected segment. Both readers successfully detected intracranial aneurysms in relatively rare locations such as basilar perforators (2/l46), distal anterior cerebral artery (DACA) (4/l46), pericallosal artery (2/l46), and azygous ACA (2/l46). Inter-observer results of the CTA location of the aneurysm are summarized in **Table (3)**.

Morphology: Among the assessed aneurysms, (96.4%) were saccular, (2.4%) were fusiform, and (1.1%) were serpentine **(fig.3).** Excellent interobserver agreement was found between both readers in the detection of aneurysm shape (K= 0.92, P=0.001) and for margins (K= 0.95, P=0.001). **Other features** such as calcification or thrombus, branch incorporation, and aneurysm orientation also show excellent inter-observer agreement. Calcification and thrombosis were detected in large and giant aneurysms **(fig.4)**. Branch incorporation was found in association with 55 aneurysms, one of them showed 3rd A2 segment incorporated ACOM aneurysm dome (ACA trifurcation), to the best of the author's knowledge this association is not reported before in the literature **(fig.5).**

Measurements: Most cases were medium-sized aneurysms (60.8%), followed by small-sized (30.1%). Both readers measured aneurysm size, neck, and dome-to-neck ratio with an excellent interobserver agreement (K= 0.89, P=0.001)**,** (K= 0.85, P=0.001), and (K= 0.98, P=0.001). Inter-observer results of CTA measurements of an aneurysm are summarized in **Table 4.**

Peri-aneurysm findings: Excellent interobserver agreement was found between both readers in detecting vasospasm in the nearby arterial segment (K= 0.91, P=0.001) and detection of the perianeurysmal cyst (K= 1.0, P=0.001). Associated vascular lesions, including arterio-venous malformation (AVM) and developmental venous anomalies (DVA) **(fig.6)**, were detected by both readers with an excellent interobserver agreement (K= 0.83, P=0.001). Vascular variations commonly affected the A1 segment, followed by PCA and MCA. Both readers detected an important bony variant in a case presented with a PCOM aneurysm in the form of a bridging sella turcica which was managed surgically by clinoidectomy **(fig.7).**

Management: Based on imaging features, 87 patients were recommended to have endovascular treatment, while surgery was recommended in 59 patients. 71.2 % of the study population underwent the recommended therapy, as 19 patients did not receive any therapy for the culprit, 66 underwent endovascular treatment, and 61 underwent surgical clipping. Only 15 % of the study population needed external ventricular drain (EVD) to manage associated hydrocephalus.

DISCUSSION

This study evaluated the interobserver reliability of CTA in the assessment of ruptured intracranial aneurysm features among 146 patients. Our results showed good to an excellent inter-observer agreement in NCCT features related to the aneurysm, aneurysm characters, measurements, and perianeurysmal information. Imaging data extracted from NCCT & CTA guided the multidisciplinary neurovascular team to better treatment approach selection.

Our results showed high sensitivity of NCCT (85%) in predicting aneurysms' location depending on blood distribution with a good inter-observer agreement regarding the Fischer scale scores for SAH. The combination of NCCT images and CTA is a valuable tool for detecting intracranial aneurysms and predicting outcomes. Aneurysm detection could be expected by assessing the distribution of SAH, the site of the largest clot, the difference in attenuation, and the presence of mural calcification. A recent study performed on patients with SAH and multiple cerebral aneurysms found that NCCT can identify the source of bleeding with high accuracy for ACA, ACom, and MCA aneurysms, especially with the presence of ICH **(10)**. Our results showed excellent inter-observer agreement for detecting acute hydrocephalus with a variable degree of acute ventricular dilation, yet only 15% of our cases need management by EVD. Our results were close to those of the study performed on 389 patients with aneurysm-associated subarachnoid hemorrhage **(11).**

We found that CTA has a high sensitivity for detecting intracranial aneurysms and avoids false-negative results. In a meta-analysis of extracted data from 8 studies, CTA had a pooled sensitivity of 99% and specificity of 94% for detecting and ruling out cerebral aneurysms **(12).** Our study had an excellent interobserver agreement for detecting the aneurysms; the first reader detected 166 aneurysms, while the second reader detected 169 aneurysms. Yang et al. revealed a similar discrepancy in number detection by two observers, as one reviewer missed three aneurysms **(8)**. The inter-observer discrepancy usually occurs in a set of multiple small aneurysms in uncommon locations, such as the distal middle cerebral artery**.** In this study, we detected mirror image aneurysms in 7 patients. Our results concord with the data obtained by a recent study by Rajogopal and colleagues **(13**).

In our study, the anterior cerebral circulation aneurysms remained the predominant location of all aneurysms detected by CTA, constituting about 94% of the anterior and 6% of the posterior circulation. ACOM aneurysm is the most common location of aneurysm in our results followed by ICA and MCA aneurysms, respectively. A similar distribution was reported by previous studies that assessed CTA versus DSA in the detection of intracranial aneurysms **(14 & 15).** Imaging is vitally important to determine the location of the aneurysm and its relationship to the surrounding anatomy. Data from many studies suggest that surgical clipping may be superior in managing anterior circulation aneurysms with low recurrent rates. In contrast, posterior circulation aneurysms may be better treated through an endovascular approach **(16).** Both readers successfully detected intracranial aneurysms in relatively rare locations, such as basilar perforators and azygous ACA. These findings aligned with prior studies stating that basilar perforator aneurysms are sporadic lesions often not recognized on initial imaging **(17 & 18)**. Similarly, azygos anterior cerebral artery aneurysm has a low incidence among intracranial aneurysms in literature ranging from 0.38 to 3.7 % **(19).**

In this study, non-saccular intracranial aneurysms were less frequent. The margins were sharp (42.7%), and the rest were lobulated. These results partially agree with Rai et al., who reported 91% of saccular aneurysms, with only 22% having lobulated margins **(15).** An irregular margin or lobulation along the margin of an aneurysm suggests rupture. It is an important observation in the setting of diffuse subarachnoid hemorrhage and multiple intracranial aneurysms when treatment is directed at the culprit aneurysm **(20).** Excellent inter-observer agreement was found in the assessment of branch incorporation and aneurysm orientation. The location of a branch to the aneurysm is a critical finding, as inadvertent occlusion of this branch during aneurysm treatment could have devastating consequences **(21)**. Therefore, it is essential to have a basic understanding of cerebral circulation and anatomical variants when interpreting CTA studies. Aneurysm orientation, especially ACOM aneurysm, is a crucial element in selecting surgical versus endovascular management. Aneurysms with a more complex surgical approach are often assessed for endovascular therapy rather than surgical management **(22).**

Excellent agreement was found in this study between both readers regarding aneurysm measurements, including size, neck diameter, and dome-to-neck ratio. As the size of the aneurysm is the most significant predictor of SAH risk, accurate measurement of the aneurysm(s) is imperative for proper management. Aneurysms larger than 12 mm had a 2.6 relative risk of poor outcomes **(23).** Kim et al. stated that intra-observer and interobserver variability in CTA were considerable in aneurysmal size measurements ranging from 12 to 18%. Therefore, follow-up size changes exceeding 20% in the aneurysm dimension should be considered a true change rather than a measurement error **(24).** In contrast to these results, another study reported a poor ability of CTA to identify aneurysm enlargement accurately in assessing an in-vitro model. However, they recommended further human studies to confirm their findings **(25)**. CTA in this study detected the neck of all saccular aneurysms by both readers. Neck dimension and neck-to-dome ratio are crucial to deciding between surgical or endovascular treatment and simple coiling or adjunctive techniques to facilitate coil embolization through wide neck, such as neck remodeling using balloons or stent-assisted embolization **(26)**.

The majority of our cases were medium-sized aneurysms (60.8%). This finding was in line with results reported by previous studies, which noted that medium-sized aneurysms were the majority of intracranial aneurysms **(14 & 15).** We also observed that the presence of thrombosis and calcification was strongly tied to aneurysm size in large-sized and giant aneurysms compared to the corresponding intra-operative details of each case. Spontaneous thrombosis of intracranial aneurysms may occur in up to 40% of giant aneurysms, eventually becoming symptomatic due to mass effect or stroke. On the contrary, spontaneous thrombosis of a non-giant aneurysm (<25 mm) is rarer **(27).** Calcification appears to be an important pre-operative indicator of poor outcomes **(28)** and should be considered when deciding treatment options for a patient with a calcified aneurysm.

Perianeurysmal findings such as vasospasm, perianeurysmal cyst, associated vascular lesions or variants, and bony landmarks or pathologic changes are essential factors that might change the treatment decision. Cerebral vasospasm and resultant delayed cerebral ischemia consider a significant etiology of morbidity and mortality in patients with aneurysmal SAH

(DCI) **(29).** CTA is a fast and reliable tool for detecting decreases in vessel caliber, as demonstrated by excellent interobserver agreement in this study.

The rarity of a perianeurysmal cyst may lead to a false diagnosis of cystic neoplasm and missing the possibility of a ruptured cerebral aneurysm. Interestingly, a perianeurysmal cyst was described in one out of 146 patients in our study. Pedro & Sih reported a case of a sizeable pontine cyst associated with an enhancing mural nodule that was misdiagnosed as a cystic neoplasm. During surgery, an aneurysm of the left PCA was identified and clipped successfully **(30)**.

Our work included four patients with associated vascular anomalies, including AVMs and DVA. The risk of intracranial hemorrhage in patients with coexisted AVM and aneurysm has been reported to be 7% annually, compared with 2%–4% annually for those with AVM alone or isolated intracranial aneurysm **(31 & 32)**. To our knowledge, the association between intracranial aneurysms & DVA is infrequent, and few case reports have been published **(33).**

In our study, both observers noted a sphenoid bone fracture and a nearby aneurysm of paraclinoid ICA secondary to head trauma. It is in agreement with results done on 5532 patients with cerebral aneurysms over 30 years by Jung et al., who state that traumatic intracranial aneurysm (TIA) after blunt brain trauma is rare and represents (0.23%) **(34).** Osseous landmarks such as the optic strut and the tuberculum sellae are considered the anatomical boundary between the intradural and extradural segments of the ICA in the paraclinoid region, which is an important factor in determining treatment strategy **(35)**.

We recommended surgical clipping or endovascular management for the culprit aneurysms based on data extracted from NCCT and CTA. 71.2 % of the study population underwent the recommended therapy. The ideal therapeutic approach for ruptured intracranial aneurysms (RIAs) is still controversial. In general, the decision on whether to clip or coil depends on several factors related to the patient, such as age and comorbidities, burden, and location of hemorrhage, aneurysm characteristics such as size, number, location, and morphology, or related procedure such as competence, technical skills and availability **(36)**. Endovascular treatment has been

associated with shorter recovery but with higher retreatment rates and slightly higher rebleeding events **(16)**. An endovascular approach is indicated in a ruptured intracranial aneurysm with comorbidity, old age, narrow neck, and a posterior circulation aneurysm. Surgery is warranted if the patient is young with an MCA aneurysm and interested in durability.

There are a few limitations to this study. First, there is no correlation with conventional angiography in all cases. Second, the general drawbacks of CT include patient exposure to ionizing radiation and the risks of iodinated contrast medium. Further studies with applications of low-dose CTA, such as the use of automatic tube current modulation and a small amount of contrast medium, are recommended. Additionally, future studies using advanced CT techniques such as higher 320 slices CT scan **(37)**, dual-energy **(38)** or source CTA, and time-resolved 4D CTA will improve temporal and spatial resolution and the image quality CTA. Also, applications of advanced vascular post-processing packages for analyzing CTA images will give comprehensive image interpretation in different planes and angles**.** We recommend further studies assessing the inter-observer agreement between neuroradiologists, neurologists, neurosurgeons, and neuro-interventionist.

Conclusion

We concluded that CTA is a promising diagnostic imaging modality for assessing intracranial aneurysm features that impact management and patient outcomes.

References

1. Turan N, Heider RA, Roy AK, et al. **Current perspectives in imaging modalities for the assessment of unruptured intracranial aneurysms: a comparative analysis and review.** World neurosurgery 2018;113:280-92.
2. Al-Smadi AS, Elmokadem A, Shaibani A, et al. **Adjunctive Efficacy of Intra-Arterial Conebeam CT Angiography Relative to DSA in the Diagnosis and Surgical Planning of Micro-Arteriovenous Malformations.** AJNR Am J Neuroradiol. 2018 Sep;39(9):1689-1695.
3. Howard BM, Hu R, Barrow JW, et al. **Comprehensive review of imaging of intracranial aneurysms and angiographically negative subarachnoid hemorrhage.** Neurosurgical focus. 2019;47:E20.
4. Elsherbini MM, Elmokadem AH, El-Morsy A, et al. **Inter-Observer Reliability of Fused Time-of-Flight MR Angiography and 3D Steady State Sequence versus 3D Contrast Enhanced Images in Evaluation of Neurovascular Compression.** Open Journal of Modern Neurosurgery 2022;12(2).
5. Ares WJ, Jankowitz BT, Tonetti DA, et al. **A comparison of digital subtraction angiography and computed tomography angiography for the diagnosis of penetrating cerebrovascular injury.** Neurosurgical focus. 2019;47:E16.
6. Yoon NK, McNally S, Taussky P, et al. **Imaging of cerebral aneurysms: a clinical perspective.** Neurovascular Imaging 2016;2:1-7.
7. Bechan RS, van Rooij SB, Sprengers ME, et al. CT angiography versus 3D rotational angiography in patients with subarachnoid hemorrhage. **Neuroradiology** 2015;57(12):1239–1246.
8. Yang ZL, Ni QQ, Schoepf UJ, et al. **Small Intracranial Aneurysms: Diagnostic Accuracy of CT Angiography.** Radiology. 2017 Dec;285(3):941-952.
9. Kizilkilic O, Huseynov E, Kandemirli SG, et al. **Detection of wall and neck calcification of unruptured intracranial aneurysms with flat-detector computed tomography.** Interv Neuroradiol. 2016;22(3):293-298.
10. Sawicki M, Kościukiewicz K, Jeżewski D, et al. **Diagnostic value of non-enhanced computed tomography in identifying location of ruptured cerebral aneurysm in**

patients with aneurysmal subarachnoid haemorrhage. Neurol Neurochir Pol 2020;54:47-53.

11. Woernle CM, Winkler KM, Burkhardt JK, et al. **Hydrocephalus in 389 patients with aneurysm-associated subarachnoid hemorrhage.** J Clin Neurosci 2013;20:824-6.

12. Feng TY, Han XF, Lang R, et al. **Subtraction CT angiography for the detection of intracranial aneurysms: A meta-analysis.** Exp Ther Med 2016;11:1930-1936.

13. Rajagopal N, Balaji A, Yamada Y, et al. **Etiopathogenesis, clinical presentation and management options of mirror aneurysms: A comparative analysis with non-mirror multiple aneurysms.** Interdisciplinary Neurosurgery (Journal name) 2019;18:100535.

14. Maniharan S, Athukorala A, Pullaperuma D, et al. **Role of digital subtraction angiography in detection of intracranial aneurysms compared with computed tomographic angiography.** Sri Lanka Journal of Radiology 2019;5(1).

15. Rai SP, ChandRan P, Pai M, et al. **Comparison of Morphology of Intracranial Aneurysms on Computed Tomography Angiography with Digital Subtraction Angiography and Intraoperative Findings-A Single Centre Experience.** J Clin Diagn Res 2019;13(1).

16. Abecassis IJ, Zeeshan Q, Ghodke BV, et al. **Surgical Versus Endovascular Management of Ruptured and Unruptured Intracranial Aneurysms: Emergent Issues and Future Directions.** World Neurosurg. 2020 Apr;136:17-27.

17. Daruwalla VJ, Syed FH, Elmokadem AH, et al. **Large basilar perforator pseudoaneurysm: A case report.** Interv Neuroradiol. 2016;22(6):662-665.

18. Enomoto N, Shinno K, Tamura T, et al. **Ruptured Basilar Artery Perforator Aneurysm: A Case Report and Review of the Literature.** NMC Case Rep J. 2020;7(3):93-100.

19. Meguins LC, Hidalgo RC, Spotti AR, et al. **Aneurysm of azygos anterior cerebral artery associated with falcine meningioma: Case Report and review of the literature.** Surg Neurol Int. 2017;8:25. Published 2017 Feb 20.

20. Wang GX, Gong MF, Wen L, et al. **Computed Tomography Angiography Evaluation of Risk Factors for Unstable Intracranial Aneurysms.** World Neurosurg 2018;115:e27-e32.

21. Kawabata Y, Nakazawa T, Fukuda S, et al. **Endovascular embolization of branch-**

incorporated cerebral aneurysms. Neuroradiol J 2017;30:600-606.

22. Chen J, Li M, Zhu X, et al. **Anterior Communicating Artery Aneurysms: Anatomical Considerations and Microsurgical Strategies.** Front Neurol 2020;11:1020.

23. Ajiboye N, Chalouhi N, Starke RM, et al. **Unruptured Cerebral Aneurysms: Evaluation and Management.** ScientificWorldJournal. 2015;2015:954954. doi:10.1155/2015/954954.

24. Kim HJ, Yoon DY, Kim ES, et al. **Intraobserver and interobserver variability in CT angiography and MR angiography measurements of the size of cerebral aneurysms.** Neuroradiology 2017;59:491-497.

25. Al Kasab S, Nakagawa D, Zanaty M, et al. **In vitro accuracy and inter-observer reliability of CT angiography in detecting intracranial aneurysm enlargement**. J Neurointerv Surg 2019;11:1015-1018.

26. Waqas M, Chin F, Rajabzadeh-Oghaz H, et al. **Size of ruptured intracranial aneurysms: a systematic review and meta-analysis.** Acta Neurochir 2020;162:1353-1362.

27. Vandenbulcke A, Messerer M, Starnoni D, et al. **Complete spontaneous thrombosis in unruptured non-giant intracranial aneurysms: A case report and systematic review.** Clin Neurol Neurosurg. 2020 Oct 19:106319.

28. Bhatia S, Sekula RF, Quigley MR, et al. **Role of calcification in the outcomes of treated, unruptured, intracerebral aneurysms.** Acta Neurochir 2011;153:905-11.

29. Kolias AG, Sen J, Belli A. **Pathogenesis of cerebral vasospasm following aneurysmal subarachnoid hemorrhage: putative mechanisms and novel approaches.** J Neurosci Res 2009;87:1-11.

30. Pedro KM, Sih IM. **Perianeurysmal Parenchymal Cyst of the Pons: A Case Report and Review of Literature.** Interdisciplinary Neurosurgery 2020;100731.

31. Chen J, Wang Y, Li P, et al. **Treatment of a giant arteriovenous malformation associated with intracranial aneurysm rupture during pregnancy: A case report**. Exp Ther Med 2016;12:1337-1340.

32. Flores BC, Klinger DR, Rickert KL, et al. **Management of intracranial aneurysms associated with arteriovenous malformations.** Neurosurg Focus. 2014 Sep;37(3):E11. doi: 10.3171/2014.6.FOCUS14165. PMID: 25175430.

33. Li J, Du S, Sun L, et al. **Hybrid Operation of a Ruptured Aneurysm Associated with a Developmental Venous Anomaly.** World Neurosurg 2018;120:63-65.

34. Jung SH, Kim SH, Kim TS, et al. **Surgical treatment of traumatic intracranial aneurysms: experiences at a single center over 30 years.** World Neurosurg 2017;98:243-250

35. Lefevre E, Apra C, Chodraui-Filho SF, et al. **Reliability of Bony Landmarks to Predict Intradural Location of Paraclinoid Aneurysms.** Clin Neuroradiol 2020;;30:843-848.

36. Steiner T, Juvela S, Unterberg A, et al. **European Stroke Organization. European Stroke Organization guidelines for the management of intracranial aneurysms and subarachnoid haemorrhage.** Cerebrovasc Dis. 2013;35(2):93-112.

37. Kim HJ, Yoon DY, Kim ES, et al. **256-row multislice CT angiography in the postoperative evaluation of cerebral aneurysms treated with titanium clips: using three-dimensional rotational angiography as the standard of reference.** Eur Radiol 2020;30:2152-2160.

38. Yun SY, Heo YJ, Jeong HW, et al. **Dual-energy CT angiography-derived virtual non-contrast images for follow-up of patients with surgically clipped aneurysms: a retrospective study.** Neuroradiology 2019;61:747-755.

TABLES:

Table 1: Imaging features considered in the management of ruptured intracranial aneurysms

	Endovascular therapy	**Surgical management**
NCCT	Absence of parenchymal hematoma.	Presence of intra-parenchymal hematoma.
Aneurysm characters	Posterior circulation aneurysms. Small aneurysm neck < 4 mm. Aneurysm diameter < 15 mm. Unilobar configuration. Multiple aneurysms. Calcification located at the aneurysm neck.	Middle cerebral and pericallosal arteries aneurysm. Aneurysm diameter > 15 mm Wide neck aneurysm > 4 mm. Abnormal configuration. Aneurysmal sac incorporating arterial branches. Presence of intraluminal thrombus.
Perianeurysmal findings	Presence of vasospasm.	Vascular variants interfere with endovascular management.

Table 2: Inter-observer agreement of CT & CTA features of aneurysm

Signs	Reader 1	Reader 2	*K*	95% CI	P value	Agreement%
NCCT findings						
SAH Fisher scale	3.47±0.6	3.33±0.4	0.84	0.78-0.85	<0.001*	89.5%
Hydrocephalus (HCP)						
Not present(N)	93	95	0.91	0.85- 0.97	<0.001*	95.9%
Present(p)	53	51				
Intraparenchymal hematoma (IPH)						
Not present (N)	105	105	1.0	1.0-1.0	<0.001*	100.0%
Present(p)	41	41				
Aneurysm features						
Number						
Total	166	169	0.95	0.89-1.0	<0.001*	98.8%
Single	126	127				
Multiple	40	42				
Size						
Small	55	57	0.89	0.83 - 0.96	<0.001*	94.7%
medium	101	102				
Large	5	5				
Giant	5	5				
Site						
Anterior	156	157	0.94	0.83-1.0	<0.001*	99.4%
Posterior	10	12				
Shape						
Saccular	160	162	0.92	0.76 - 1.0	<0.001*	99.4%
Fusiform	4	4				
Serpentine	2	2				
Blister	0	1				

Margin						
sharp	71	75	0.95	0.90 - 0.99	<0.001*	97.6%
lobulated	95	94				
Thrombus						
Positive	6	9	0.82	0.65 - 0.99	<0.001*	97.6%
Calcification						
Positive	9	9	1.0	1.0-1.0	<0.001*	100.0%
Branch incorporation						
Positive	50	55	0.90	0.83 - 0.97	<0.001*	95.9%
Orientation			0.95	0.91- 0.97	<0.001*	96.5%
Perianeurysmal findings						
Vasospasm						
Positive	21	25	0.90	0.81 - 0.99	<0.001*	97.6%
Perianeurysmal cyst						
Positive	1	1	1.0	1.0-1.0	<0.001*	100.0%
Other vascular lesions						
Positive	2	4	0.82	0.59 - 1.0	<0.001*	98.8%
Bony relations						
Positive	23	26	0.88	0.78 - 0.98	<0.001*	97.0%
Bone fracture (F)	1	1				
Vascular variant						
Present(p)	84	88	0.89	0.83 - 0.96	<0.001*	94.9%
Overall agreement			0.95	0.94-0.96	<0.001*	97.8%

Table 3: Inter-observer agreement of CTA locations of aneurysm

Parent artery	**Reader 1**	**Reader 2**
ACOM	73	73
ACA	5	6
RT ICA	20	20
LT ICA	16	16
RT MCA	21	22
LT MCA	20	20
Basilar	8	9
LT PCA	1	1
RT .Vertebral	1	1
LT SCA	0	1
K	**95% CI**	**P value**
0.97	0.87-1.0	<0.001*
Arterial segment	**Reader 1**	**Reader 2**
ACOM- Lt ACA complex	36	36
ACOM- Rt ACA complex	34	34
ACOM proper	3	3
A1	1	1
A2		
RT	1	1
LT	0	1
Azygous	2	2
A3	1	1

MCA bifurcation		
RT	14	14
LT	15	15
M1		
RT	4	4
LT	3	3
M2	3	
RT		3
LT	2	2
M4	0	1
PCOM		
RT	12	12
LT	9	9
ICA Terminus	4	
RT		4
LT	2	2
Cavernous ICA		
RT	4	4
LT	5	5
Basilar		
Tip	4	4
Mid	2	3
Perforators	2	2
Rt **V4**	1	1
LT **SCA**	0	1
Lt **P1**	1	1
K	**95% CI**	**P value**
0.97	0.87-1.0	<0.001*

Table 4: Inter-observer agreement of CTA measurements of aneurysm

	Size		Dome		Neck		Dome / neck ratio	
	Reader 1	**Reader 2**	**Reader 1**	**Reader 2**	**Reader 1**	**Reader 2**	**Reader 1**	**Reader 2**
Mean	7.4	7.4	3.7	3.6	2.7	2.7	1.3	1.3
Median	6.0	6.0	3.0	3.0	2.3	2.3	1.2000	1.2
Std. Deviation	5.44	5.47	3.2	3.1	2.1	2.1	0.8	0.8
Minimum	1.8	1.8	1.0	1.0	1.0	1.0	0.2	0.2
Maximum	40.0	42.0	22.0	22.0	20.0	20.0	4.7	5.6
ICC	0.97		0.97		0.96		0.98	
95% CI	(0.96-0.98)		(0.96-0.97)		(0.95-0.97)		(0.97-0.98)	

FIGURES

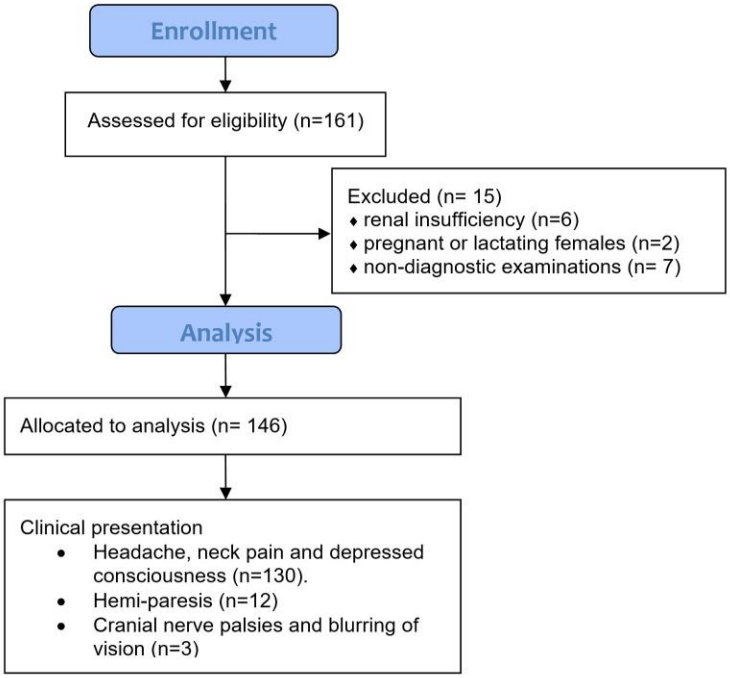

Figure (1): Flow chart of the study.

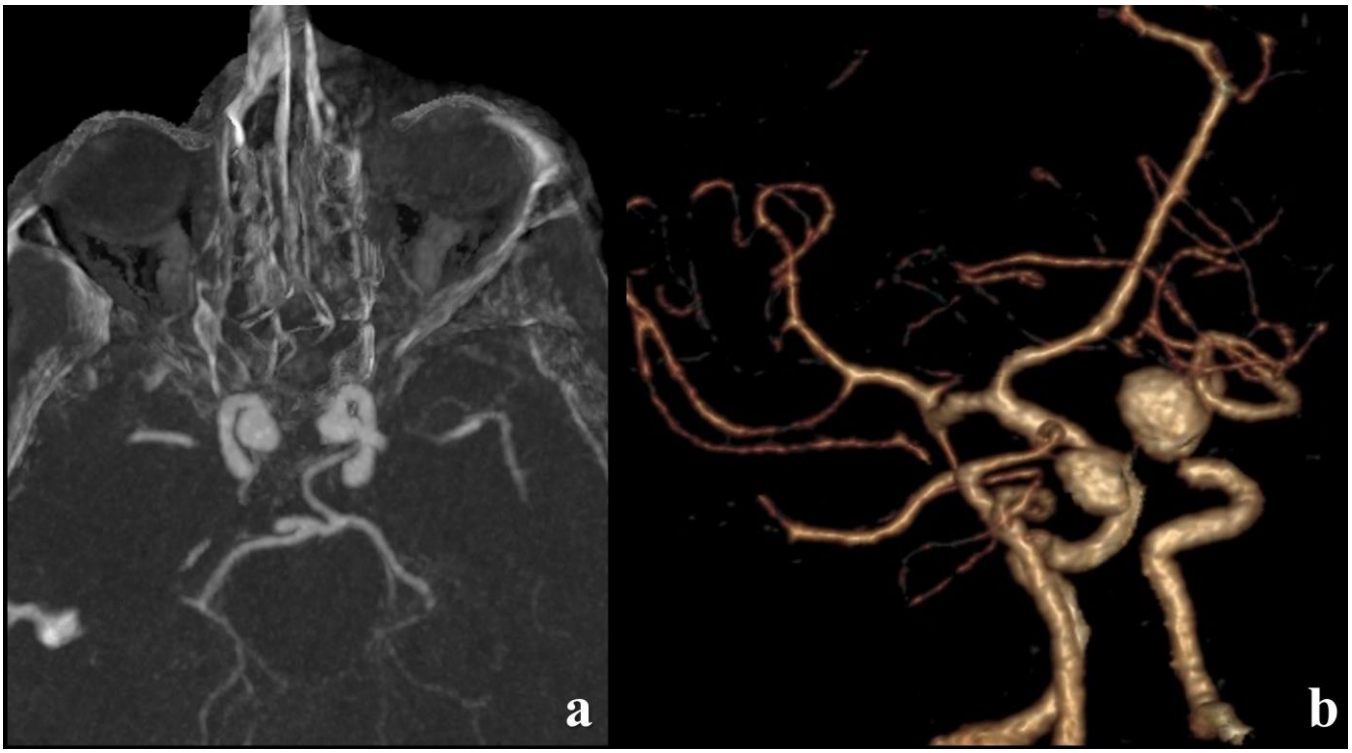

Figure (2): Mirror image intracranial aneurysms. (a & b) axial CTA in MIP projection and 3d CTA for mirror image ICA aneurysms.

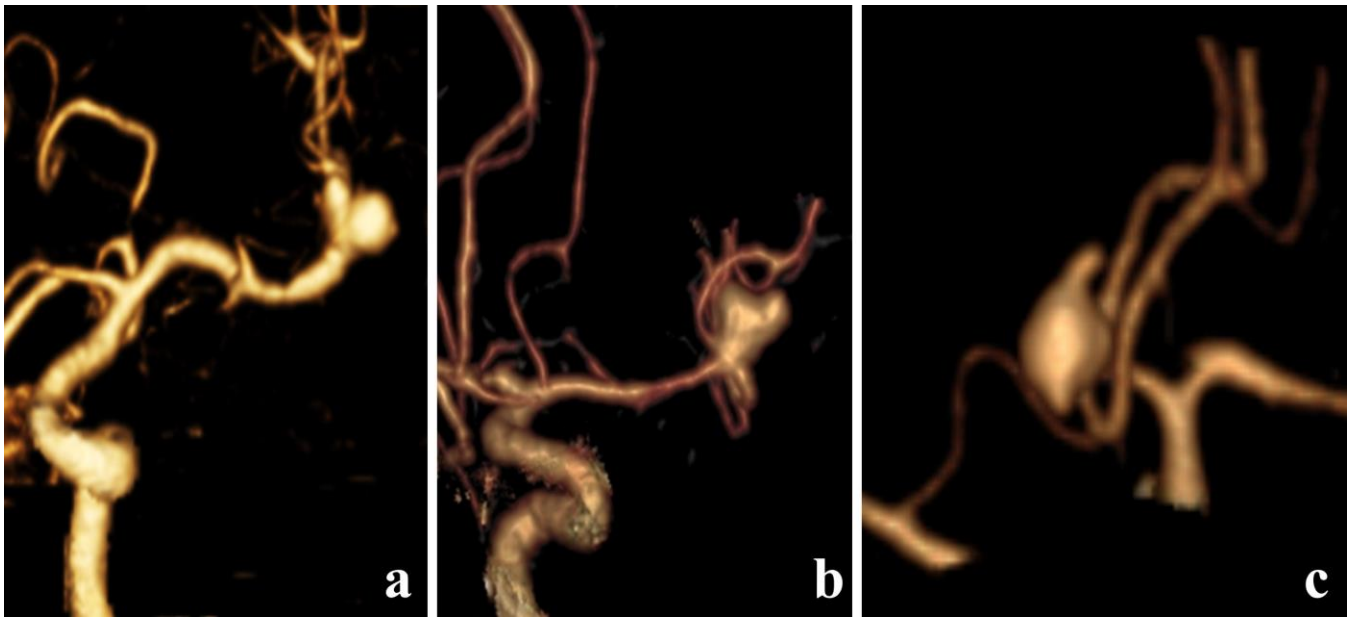

Figure (3): Morphology of intracranial aneurysms. (a) 3D-CTA for saccular aneurysm at MCA bifurcation with smooth margins. (b) 3D-CTA for saccular aneurysm at MCA bifurcation with daughter sac. (c) 3D-CTA for ACOM saccular aneurysm with multiple blebs.

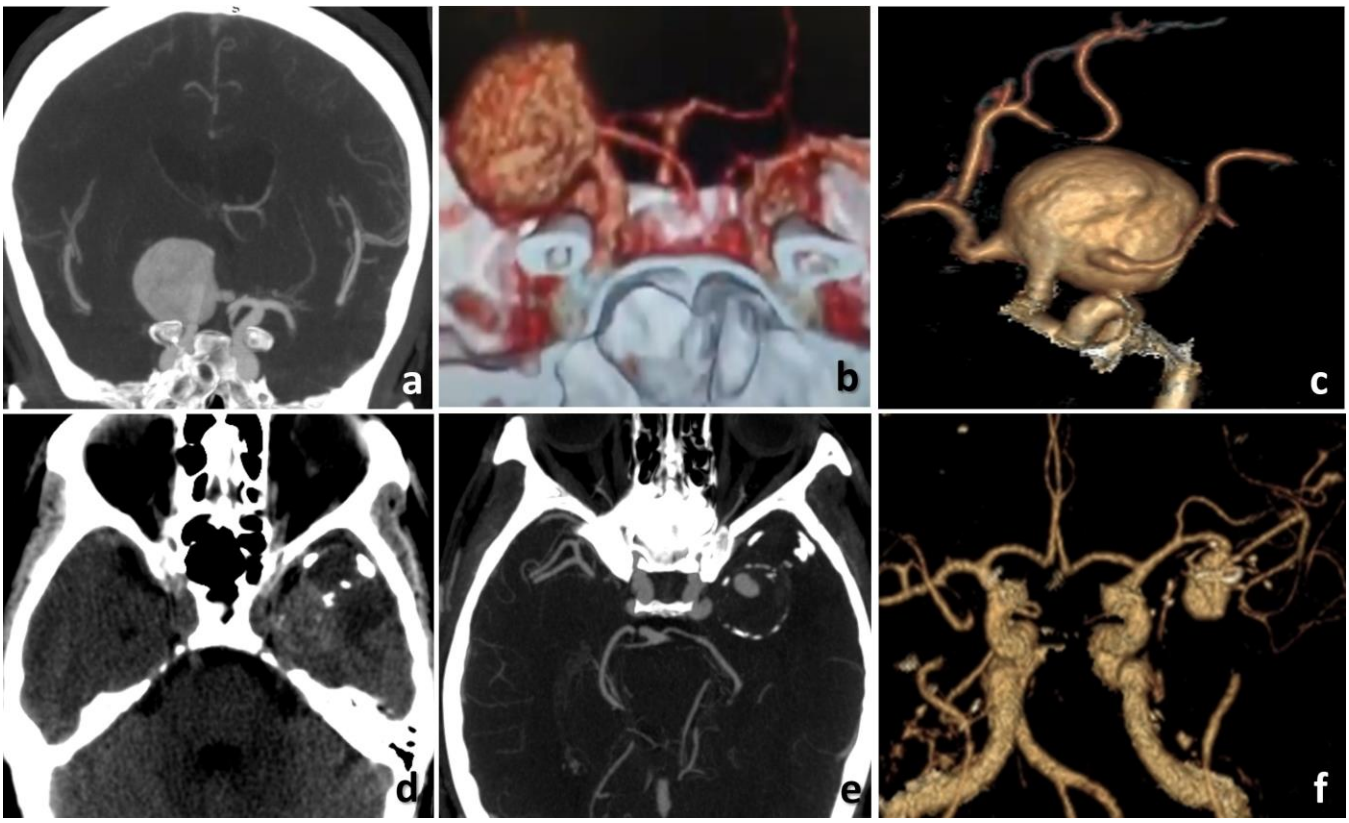

Figure (4): Giant intracranial aneurysms. (a) axial CTA in MIP projection, (b & c) 3D-CTA for giant saccular aneurysm arising from right ICA and incorporating the origin of ACA and MCA. (d) NCCT for another patient shows a well defined lobulated lesion of mixed density in the left temporal lobe with foci of peripheral calcification, (e) MIP-CTA axial image shows giant partially thrombosed saccular aneurysm of left MCA and (f) 3D –CTA image shows a patent portion of left MCA aneurysm.

Figure (5): Anatomical variants with intracranial aneurysms. (a) Sagittal reformatted MIP-CTA and (b) 3D-CTA for a saccular aneurysm at ACA trifurcation.

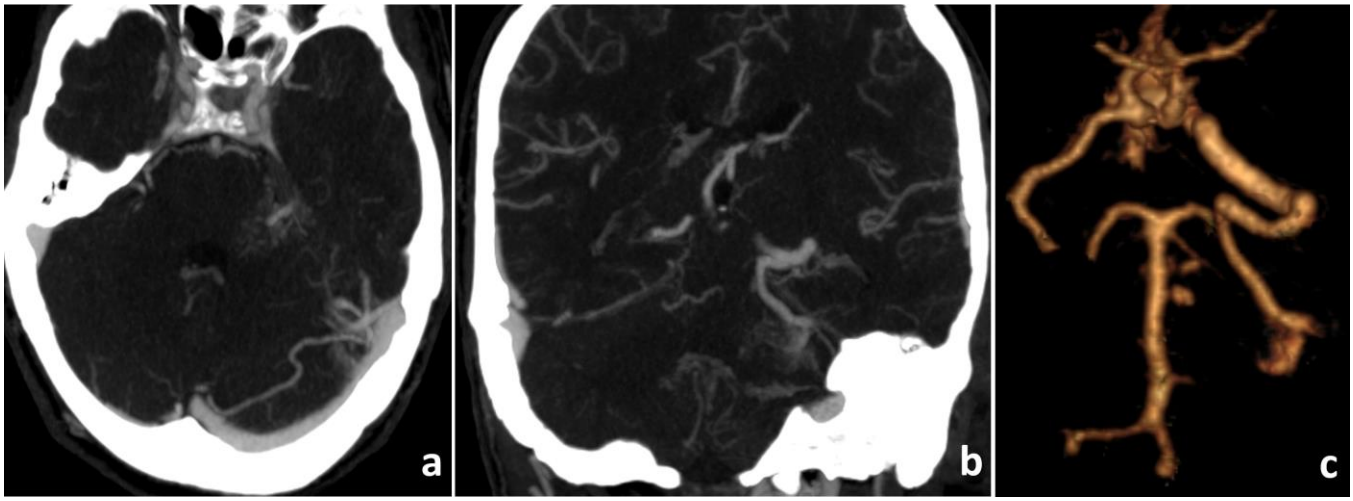

Figure (6): Vascular malformation with intracranial aneurysms. (a) axial MIP-CTA shows a small saccular aneurysm that arises from the left basilar artery perforators. (b) Coronal reformatted MIP-CTA shows left cerebellar DVA drains into the left sigmoid sinus. (c) 3D-CTA shows the basilar perforator aneurysms and the left cerebellar DVA.

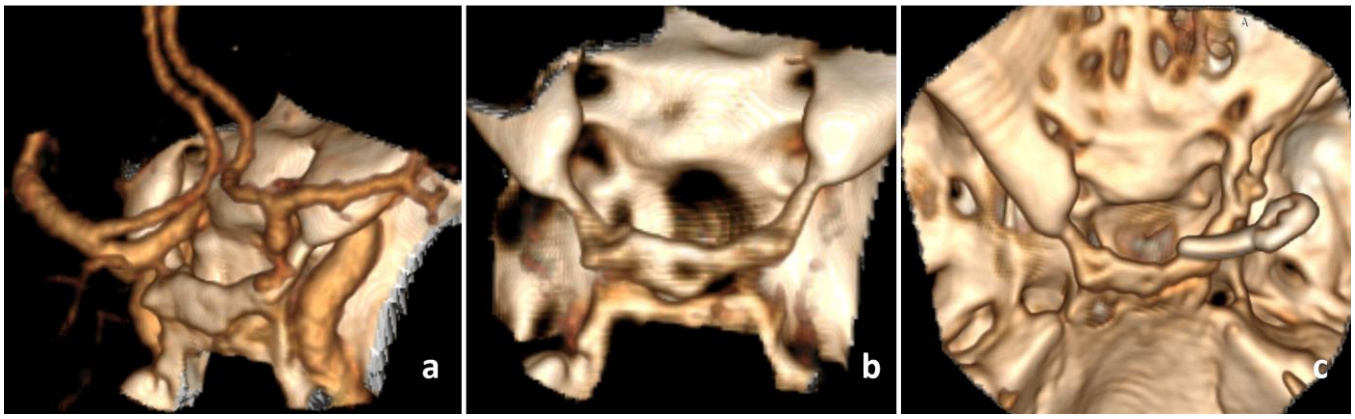

Figure (7): Bony landmarks related to the aneurysm. (a) 3D-CTA shows a PCOM aneurysm close to the anterior clinoid process. (b) 3D-CT for the skull base shows bridging sella and bony fusion. (c) Post-operative 3D-CT shows partial clionoidectomy and metallic clip.